Impact of antibiotic-induced depletion of gut microbiota and selenium supplementation on plasma selenoproteome and metal homeostasis in mice model

Belén Callejón-Leblic[a], Marta Selma-Royo[b], María Carmen Collado[bΣ], Nieves Abril[cΣ], Tamara García-Barrera[aΣ*]

[a]Research Center of Natural Resources, Health and the Environment (RENSMA). Department of Chemistry, Faculty of Experimental Sciences, University of Huelva, Fuerzas Armadas Ave., 21007, Huelva, Spain; [b]Institute of Agrochemistry and Food Technology-National Research Council (IATA-CSIC), Department of Biotechnology, Agustin Escardino 7. 46980 Paterna, Valencia, Spain, [c]Department of Biochemistry and Molecular Biology, University of Córdoba, Campus de Rabanales, Edificio Severo Ochoa, E-14071, Córdoba, Spain. Σ senior authors;

*tamara@dqcm.uhu.es

Abstract

Selenium (Se) is a micronutrient involved in important health functions and it has been suggested to shape gut microbiota. Limited information on the Se assimilation by gut microbes and the possible link with selenoproteins are available. For this purpose, conventional and gut microbiota depleted BALB/c mice were fed a Se-supplemented diet. The absolute quantification of mice plasma selenoproteins was performed for the first time using heteroatom-tagged proteomics. Gut microbiota profile was analyzed by 16S rRNA gene sequencing. Se-supplementation modulated the concentration of the antioxidant glutathione peroxidase and the Se-transporter selenoalbumin as well as the metal homeostasis, being influenced by microbiota disruption, which suggests an intertwined mechanism. Se also modulated microbiota diversity, richness, and increased the relative abundance some health-relevant taxa (*e.g.* Families *Christensenellaceae, Ruminoccocaceae and Lactobacillus* genus). This study demonstrated the potential beneficial effects of Se on gut microbiota, especially after antibiotic-treatment and the first associations between specific bacteria and plasma selenoproteins.

Keywords: selenoproteins, microbiota, chemical speciation, heteroatom-tagged proteomics, ICP-MS.

Introduction

The role of selenium (Se) in biology has been extensively reviewed due to its antioxidant character and the potential relevance to certain diseases such as cancer[1] or cardiovascular disease.[2] Thus, there is a great interest into develop Se-enriched functional foods and nutraceuticals.[3] The main source of Se is the diet, but the relationship between status and dietary intake of this micronutrient is close to a U-shape, where adverse effects are derived from deficiency and excess, being the Se-essentiality conditioned to a narrow range of concentration.[4] This means that Se-enriched nutraceuticals and functional foods should control the bioavailable concentration of this element, however, the chemical form of Se used is also of importance.[5] The most commonly marketed Se-enriched product is yeast *Saccharomyces cerevisiae*, but other functional foods have also been proposed such as *Chlorella sorokiniana.*[6] Moreover, minerals as Se can shape the colonization of gut microbiota, deeply affecting the host health.[7] Accumulating data is demonstrating the pivotal role of gut microbiota on human health. Gut dysbiosis has been associated with high risk of metabolic and inflammatory alterations.[8] Gut microbiota, in turn, can act as a barrier or modulator for nutrients, toxics and pollutants.[9] Nowadays, there is a growing interest in the design of dietary strategies for the modulation and the re-building of microbiota.[10] Few works have reported the impact of a Se-supplemented diet gut microbiota because most of them have been only focused on Se-deficient diet.[11,12] Zhai *et al* concluded that supranutritional Se intake in the form of Na_2SeO_3 can optimize the gut microbiota for protection against intestinal dysfunctions in specific pathogen-free mice[9], and Liu *et al* reported a partial restore of the abundance of gut flora after Se-treatment of rats exposed to methylmercury.[13] Although the beneficial functions of Se for gut microbiota has been attributed to selenoproteins and selenometabolites[9], little is known about the effect of Se-supplementation on host plasma

selenoproteome and the potential link with gut microbiota. Likewise, the absolute quantification of plasma selenoproteins and correlation with specific bacteria have not been reported before and few works determined the expression profiles of certain selenoproteins after Se-supplementation in conventional (CV) and germ free (GF) mice by enzymatic activities[11] or western blot complemented with quantitative polymerase chain reaction (PCR).[14]

In this sense, the aim of this study was the absolute quantification, by the first time, of plasma selenoproteins in Se-supplemented CV and mice with microbiota depleted by antibiotics as well as their associations with specific bacteria. Selenoproteins have been determined using a highly sensitive and selective analytical technique namely heteroatom-tagged proteomics and the gut microbiota taxonomy by 16S rRNA gene sequencing. The impact of Se-supplementation on gut microbiota diversity, richness and composition has been determined in both mice models. We also studied the influence of Se-supplementation and gut microbiota disruption in metal homeostasis and established the correlations between their concentration and the relative abundance of specific bacteria.

Material and methods

Animals, Experimental Design and Dosage Information

Male *Mus musculus* mice (inbred BALB/c strain, 8 weeks, 23-25 g) were purchased from Charles River Laboratories (Spain). The experiments were carried out in the Animal Experimentation Service of the University of Cordoba (SAEX-UCO), in a conditioned laboratory with controlled temperature (25 ±2 °C) and photoperiod (12:12 h). The mice had free access to food and water, which were changed every second day to maintain their quality and weighed to calculate the actual ingested doses of experimental compounds. Forty mice were randomly

divided into four groups (10 mice per group). The reference group (group C) was fed a rodent diet for three weeks (around 0.20 mg Se kg^{-1} chow). The group C-Se was fed the regular rodent diet for a week and then, a Se-enriched diet containing 0.65 mg Se kg^{-1} chow as sodium selenite for the last two additional weeks. This non-toxic Se concentration was selected according to literature[15,16] and our previous works about the influence of Se in mice metabolism and its antagonistic action against toxic compounds.[17,18] Mice in the Abx and Abx-Se groups received the regular diet and water containing a cocktail of broad-spectrum antibiotics (ampicillin 1 g L^{-1}, neomycin 1 g L^{-1}, metronidazole 1 g L^{-1}, vancomycin 0.5 g L^{-1} and the antifungal amphotericin B 10 mg L^{-1}) during the first week. They were fed the regular diet for three weeks (Abx) or for one week followed by the Se-supplemented diet for the two additional weeks (Abx-Se). The selection of this cocktail was also based in the literature.[19–21] Figure 1 shows the experimental design of the study. At the end of the experimental time, mice were anesthetized by isoflurane inhalation, exsanguinated by cardiac puncture and dissected using a ceramic scalpel. All animals received humane care in compliance with animal care guidelines and use of the European Community. The investigation was performed with the consent of the Ethical Committee of the University of Córdoba (Spain) (Code Num. 02-01-2019-001).

Biological Samples

Blood samples were collected in heparinized tubes that were centrifuged (3000 *g*, 10 min, room temperature) within 30 minutes after blood collection to obtain the plasma. Large intestinal content was collected and flash frozen in liquid nitrogen. Both, plasma aliquots and gut samples were stored at -80ºC until analysis.

Antibiotic Cocktail, Standard Solutions and Reagents

Ammonium acetate ($NH_4CH_3CO_2$), sodium selenite (Na_2SeO_3), the antibiotics ampicillin, neomycin, metronidazole vancomycin and the antifungal amphotericin B were purchased from Sigma-Aldrich, (Steinheim, Germany). Trace metal grade nitric acid (HNO_3) was obtained from Fisher Scientific (Leicestershire, UK). Enriched ^{74}Se for isotopic dilution analysis was obtained from Cambridge Isotope Laboratories (Andover, MA). The BCR-637 human serum certified reference material (CRM) was purchased from the Institute for Reference Materials and Measurements (IRMM, Geel, Belgium). Serum Control for Trace Element lyophilized for Trace Elements, Level II was obtained from Clinchek, RECIPE (Munich, Germany). Water was purified with a Milli-Q Gradient system (Millipore, Watford, UK). DNA Purification Kit was obtained from Macherey-Nagel (Duren, Germany), Master-Pure DNA extraction Kit from Epicentre (Madison, WI, US) and NextEra Index Kit from Illumina (San Diego, CA, United States).

Speciation of Selenoproteins in Mice Plasma

Speciation of selenoproteins in plasma from mice was carried out by a column switching method coupled to inductively coupled plasma mass spectrometer (ICP-MS) as described previously.[22] Briefly, before the analysis, plasma samples were filtered using Iso-Disc filters of polyvinylidene difluoride (PVDF) (20 mm of diameter and 0.45 μm of pore size). Then, 100 μL of plasma were injected into a high performance liquid chromatograph (HPLC) model 1260 Infinity Quaternary LC (Agilent Technologies) connected to two 5 ml HiTrap ®Desalting Columns (GE Healthcare, Uppsala, Sweden) and two affinity columns of heparin-sepharose (HEP-HP) and blue-sepharose (BLU-HP) (GE Healthcare, Uppsala, Sweden). Ammonium acetate was used for the preparation of mobile phases A (0.05 M, pH=7.4) and B (1.5 M, pH= 7.4) and the flow-rate was set at 1.3 ml min^{-1}. The columns were interconnected using a six-way valve and finally, they were coupled to

a triple quadrupole inductively coupled plasma mass spectrometer (ICP-QQQ-MS) model Agilent 8800 Triple Quad (Agilent Technologies, Tokyo, Japan) through a Micromist nebulizer (Glass Expansion, Switzerland). The HEP-HP column is able to retain selenoprotein P (SEPP1), while the BLU-HP column retains both SEPP1 and selenoalbumin (SeAlb). To separate the selenoproteins, we applied two working modes: (i) Mode 1 (from 0 to 20 min, mobile phase A), plasma sample pass through the whole system 2D-SEC-SEC-AF(HEP-HP)xAF(BLU-HP)-ICP-MS allowing the elution of plasma glutathione peroxidase (GPx) and selenometabolites at 4 and 8 minutes respectively and the retention of SEPP1 in the HEP-HP column and SeAlb in BLU-HP column; (ii) Mode 2 (from 20 to 24 min, mobile phase B), SEPP1 elutes at 20.5 minutes and SeAlb is isolated in BLU-HP column; (iii) Mode 3 (from 24 to 40 min, mobile phase B), SeAlb is released and can elute at 25 minutes. The absolute quantification of selenocompounds was carried out using the species unspecific isotopic dilution analysis (SUID). To this end, a flow-rate of 0.1 mL min^{-1} of Se-enriched standard (^{74}Se Cambridge Isotope Laboratories, Andover, MA, USA) was introduced into the system after the chromatographic separation (post-column) using a T shape connector. The instrumental conditions for the speciation of selenoproteins have been previously described.[22] The quality of the analytical method (Table S1) was verified using the human serum BCR-637 certified reference material (CRM) (Institute for Reference Materials and Measurements, IRMM, Geel, Belgium).

Total Determination of Elements in Mice Plasma

Total elemental analysis of Al, V, Cr, Mn, Fe, Co, Ni, Cu, Zn, As, Se, Mo, Cd, Sb, Tl and Pb was performed on an Agilent 8800 ICP-QQQ-MS. Before the analysis, plasma samples were 5-fold diluted with water and filtered using PVDF filters. For the quantification of the majority of elements (except for Mo and Sb), a multi-element calibration standard solution (10 mg $L^{-1,}$

Agilent Technologies) was used to prepare the calibration curves from 0 to 250 ng g^{-1}. Individual standards solutions of Mo and Sb were necessary to determine the concentration of these elements in plasma samples. In addition, 0.1 mg L^{-1} of rhodium was used as internal standard. A Serum Control (Trace Element, Level II, RECIPE) was treated and analyzed with the same conditions as samples to check the variability and reproducibility of the analysis (Table S2). Instrumental conditions for the analysis are also described in Supplementary Material.

Determination of the Gut Microbiota Profile in Mice

Total DNA was extracted from the frozen fecal material (approx. 100 mg) using the Master-Pure the DNA extraction Kit (Epicentre, Madison, WI, US) following the manufacturer's instructions with the following modifications: samples were treated with lysozyme (20 mg mL^{-1}) and mutanolysin (5 U mL^{-1}) for 60 min at 37ºC and a preliminary step of cell disruption with 3-μm diameter glass beads during 1 min at 6 m s^{-1} by a bead beater FastPrep 24-5G Homogenizer (MP Biomedicals) as described elsewhere.[23] Purification of the DNA was performed using DNA Purification Kit (Macherey-Nagel, Duren, Germany) according to manufacturer's instructions and DNA concentration was measured using Qubit® 2.0 Fluorometer (Life Technology, Carlsbad, CA, US) for further analysis.

Gut microbiota profile was determined by V3-V4 variable region of the 16S rRNA gene sequencing following Illumina protocols. Briefly, a multiplexing step was conducted by the NextEra Index Kit (Illumina, San Diego, CA, United States) and amplicons were checked with a Bioanalyzer DNA 1000 chip (Agilent Technologies, Santa Clara, CA, United States). Libraries were sequenced using a 2x300 bp paired-end run (MiSeq Reagent kit v3) on a MiSeq-Illumina platform (FISABIO sequencing service, Valencia, Spain) according to manufacturer instructions. Controls during DNA extraction and PCR amplification were also included and sequenced.

Residual adaptors were removed from the raw sequences by use of Trimmomatic software.[24] DADA2 pipeline was used to achieve quality filtering, sequence joining and chimera removal.[25] Taxonomic assignment, including the specie level classification, was performed by using Silva v132 database.[26,27] Samples with less than 1000 reads were removed from the study. Taxa present in a relative abundance less than 0.01% and those present in less than 3 times in at least 20% of the samples were also filtered. Furthermore, sequences classified as Cyanobacteria and Chloroplast were removed from the final dataset as they represent potential contaminants.

Statistical Analysis

One-way ANOVA and Tukey test for multiple comparisons were applied to the results using STATISTICA 8.0 from StatSoft. Spearman correlations between selenoproteins, metals and microbiota (phylum and genus level) were determined using R Software Package Hmisc (4.0.2 version)[28]. For the microbiota analyses, Calypso web platform v. 8.56[29] was used with total sum normalization for the statistical analysis, multivariate test and data mining. Alpha-diversity metrics (Chao1 and Shannon indexes) were obtained at amplicon sequence variant (ASV) level after rarefaction to the minimum reads number (93,525 reads). Permutational multivariate analysis of variance using Bray-Curtis distance (Adonis) at ASV level was performed and the visualization of the multivariate analysis was assessed by Redundancy Discriminant Analysis (RDA). Data were classified by metadata factors and differences in relative abundance were evaluated by Wilcoxon test with False Discovery test Rate (FDR) for multiple test correction. Comparisons 2x2 of microbiota composition at phylum and genus level were performed by the DESeq2 approach with the false discovery rate correction. The level of statistical significance for all tests was fixed to $p < 0.05$.

Results and Discussion

Herein, we report the impact/effect of Se-enriched diet on selenoproteins and total Se in mice plasma in presence and absence of antibiotics to induce gut microbiota depletion. The estimated daily ingest of Se was about 40 μg kg^{-1} bw for mice fed the regular diet, and about 120 μg kg^{-1} bw for the mice fed the Se-enriched diet. Popular Se supplement products, including both organic and inorganic chemical forms, usually do not exceed 200 μg/day (about 3 times the requirement)[30] to avoid the inhibitory or toxic effect exerted by Se at a high dose.[31] Since the regular mouse chow diet in our study contains about 0.20 mg Se kg^{-1} chow, we decided to formulate a Se-enriched diet containing 0.65 mg Se kg^{-1} chow (about 3 times the regular Se ingest). As previously reported,[21] we selected a cocktail containing the antibiotics ampicillin, neomycin, metronidazole, vancomycin and the antifungal amphotericin B to deplete the gut microbiota. The estimated daily ingest of antibiotics during the pretreatment by mice in Abx and Abx-Se groups was 200 mg kg^{-1} bw of ampicillin, neomycin and metronidazole, 100 mg kg^{-1} bw of vancomycin and 2 mg kg^{-1} bw of amphotericin B. No lethality was observed during the different phases of treatment, but the antibiotics pretreatment caused a severe weight lost in mice, which was quickly recovered after moving to the treatment phase.

Impact of Selenium Supplementation on Plasma Selenoproteome is affected by Microbial Antibiotic Disruption

Quantification of plasma selenoproteins and selenometabolites was performed by unspecific isotopic dilution analysis (IDA) using the chromatographic column switching method 2D-SEC-SEC-AF(HEP-HP)xAF(BLU-HP)-ICP-MS described previously. This analytical method allows the absolute quantification of selenoproteins using a heteroelement (an atom different to C, H, N, O or F, *e.g.* Se) of the biomolecule as a "tag" in a sensitive and selective detector such as ICP-

MS.[32] Thus, using heteroatom-tagged proteomics, the absolute concentration of selenoproteins (as Se) can be determined instead of the enzymatic activity or their relative concentration typically used in protein analysis.

Figure 2 shows the mass flow chromatograms of (a) the BCR-637 serum certified reference material spiked with 50 ng g^{-1} of sodium selenite, and (b) a mice plasma sample. Levels of selenometabolites (which elute in a single peak after GPx) were lower than the detection limit in all the samples. In the bloodstream, SEPP1 accounts for >50% of Se, followed by SeAlb (~15-20 %) and GPx (~15-20 %)[33] that is in good agreement with our results. These three selenoproteins are the most commonly used markers for the assessment of Se status in human plasma/serum[34]. Under our knowledge, SeAlb has not been previously reported in microbiota studies after Se-supplementation. SeAlb transports Se to the liver for the production of the majority of selenoproteins and delivery of metabolites to the plasma.[35]

A one-way ANOVA analysis was carried out to determine the statistical significance of the differences observed among the four experimental groups C, C-Se, Abx and Abx-Se regarding to both the total Se and plasma selenoproteins concentrations (Table 1). The average concentration of SEPP1 and total Se did not change significantly when comparing the groups under study, suggesting that the main role of SEPP1 (*i.e.* the transport of Se from the liver to other organs or prevention of neurotoxicity[36]) did not resulted altered neither by Se-supplementation or antibiotics-induced microbiota depletion, at the studied levels. However, as commented in next sections, this protein and total Se correlate with specific bacteria in the different groups showing their interplay with gut microbiota. In contrast, the ANOVA analysis showed significant increases of GPx and SeAlb levels after Se-supplementation of CV mice diet (groups C-Se vs C). The increases in GPx and SeAlb levels were also significant after microbiota depletion (Abx vs

C) and when analyzing the combined effect of Se-supplementation and microbiota depletion (Abx-Se vs C) (Table 1). No significant changes in GPx and SeAlb abundances were observed in the comparisons between Abx-Se vs Abx or Abx-Se vs C-Se. Thus, Se-supplementation affected GPx concentration in both CV and Abx, indicating an increase in the antioxidant function of host[37]. The reason for the increase in the levels of GPx and SeAlb after depletion of the microbiota by antibiotics (Abx vs C) is less obvious. It has been reported that about one quarter of all bacteria express selenoproteins and therefore sequester some Se for optimal growth and their normal metabolic functions.[14] The explanation could be that the bacteria that grow after antibiotic treatment are less able to sequester Se, thus decreasing competition with the host. Then, a higher Se availability would lead to higher levels of GPx and SeAlb in the Abx mice. Figure 3 shows a model map of the mechanism underlying the potential beneficial effects of Se in the conditions with and without antibiotics. In agreement with our data, it has been also showed that GF mice fed Se diets had an expression profile of certain selenoproteins similar to control mice, but showed higher activity of GPx and methionine-R-sulfoxide reductase 1 in the liver, suggesting the partial use of Se by the gut microbes.[14]

Impact of the Selenium Supplementation and Microbiota Depletion on Trace Elements Homeostasis is affected by Microbial Antibiotic Disruption

The concentrations of several metals and metalloids (Al, V, Cr, Mn, Fe, Co, Ni, Cu, Zn, As, Mo, Cd, Sb, Tl and Pb) determined by ICP-QQQ-MS on mice plasma from the different groups studied in this work (C, C-Se, Abx and Abx-Se) are shown in Table 2. Fold changes between groups are also listed in Table 2 and only significant *p*-values are shown. The homeostasis of elements has a key importance on human health since numerous antagonistic and synergistic interactions between elements have been described in the literature [38]. In fact, Se is a well-known

antagonist against a great number of pollutants including mercury, arsenic and organic compounds.[38] However, few studies have described metal homeostasis in mice after Se-supplementation[39,40] and only Kasaikina *et al* have reported the influence of Se status and gut microbes to other elements in GF mice organs.[14] These authors only found higher levels of Cd in the liver from GF mice suggesting a possible antagonistic role of the gastrointestinal microbiota against this element[14]. Thus, this is the first time that statistically significant differences have been found in the plasma multielemental profile after Se supplementation, especially in mice with microbiota depleted by antibiotics. Se supplementation increased the levels of Al and Mo in plasma from conventional mice (C-Se vs C) and Zn in mice with depletion of microbiota by antibiotics (Abx-Se vs Abx). Remarkably, most of the differences were found in microbiota depleted mice fed Se-supplemented diet (Abx-Se vs C-Se), which may indicate that in the absence of microbiota, the influence of Se in metal homeostasis is completely different. Thus, the concentrations of Al, V, Cu and Co were significantly lower in Abx-Se against C-Se, while the concentration of Co diminished and Zn increased significantly against C (Abx-Se vs C). These results may indicate that metal homeostasis is affected by Se-supplementation and could be linked with gut microbiota, as significant differences were observed between conventional and antibiotic-depleted microbiota groups. This is in good accordance with the results previously discussed about the influence of Se-supplementation on plasma selenoproteome.

Impact of Antibiotic and Selenium Supplementation on the Gut Microbiota

Microbiota depletion by antibiotics exposure and Se-supplementation had a significant impact on the gut microbiota profile (Adonis with Bray Curtis distance R^2=0.246 and p=0.0003) (Figure 4a). This effect was also confirmed by a multivariate redundant discriminant analysis (RDA) (F=2.56 and p=0.001) (Figure 4b).

Se and antibiotic exposure had an impact on the alpha-diversity indexes as microbial diversity ($p = 0.019$, Shannon index) and richness ($p = 0.006$, Chao1 index) (Figure 4c, d). Those differences were not influenced by sequencing coverage as no differences were found between numbers of sequences per group (Figure S1). Abx mice group showed the lowest microbial diversity and richness compared to the other groups; however, Se-supplementation (Abx-Se) modulated the antibiotic impact in terms of the microbial diversity and richness ($p<0.05$). No differences in alpha diversity indexes were observed in the conventional mice groups with and without Se-supplementation (C-Se vs C).

In terms of relative abundances, Se-supplementation and antibiotic-depletion had a relevant impact on microbiota composition (Figure 4 and S2).

No differences were found in the main phyla as Firmicutes, Bacteroides and Verrucomocrobia between groups. However, other studies have reported significant differences in Firmicutes levels in mice fed Se-supplemented diet.[41] Proteobacteria was higher in C-Se group than the other groups showing an increase in this pro-inflammatory phylum[42] in agreement with other studies that reported a significant increase of its abundance in mice fed Se-enriched *C. megacephala larvae*.[43] We also observed an increased abundance of Tenericutes phylum in Se-supplemented groups, both C-Se and Abx-Se, compared to the non-supplemented groups. In agreement with our data, it has been described higher levels of Tenericutes in beef calves receiving Se-biofortified alfalfa.[44] Moreover, Deferribacteres phylum members, concretely *Denitrovibrio acetiphilus N2460(T)*, has been linked with the capability of growing with dimethyl sulfoxide, selenate or arsenate provided as a terminal electron acceptor, and 15 genes has been identified that could possibly encode respiratory reductases for these compounds.[45] In fact, *Deferribacter desulfuricans* has also been reported to grow at the expense of dissimilatory

reduction of As(V) to As(III).[46] In addition to As(V), D. desulfurican strain MPA-C3 utilizes NO^{3-}, Se(VI), Se(IV), fumarate and Fe(III) as electron acceptors and acetate, pyruvate, fructose and benzoate as sources of carbon and energy. In our data, higher abundance of Deferribacteres members has been identified in Se-supplemented groups, being higher in C-Se than in Abx-Se.

To explore the variation of the microbial community composition between groups, we performed LEfSe tests to detect differences in relative abundance of bacterial taxa across fecal samples (Figure 4e and S3). LEfSe analysis showed a statistically significant enrichment of the *Deferribacteriaceae*, *Eubacteriaceae* and *Christensenellaceae* families in the C-Se group, while the *Tannerellaceae* and *Caulobacteraceae* families were enriched in Abx group (Figure 4e). Specifically, the distinction was due to a higher abundance of members of the Deferribacteres phylum in Se group as compared to the other groups ($p=0.001$) (Figure 4f).

At the genus level, higher abundances of *Lactobacillus* ($p=0.001$) and *Flavonifactor* ($p=0.002$) were observed in conventional groups (C and C-Se) and in Abx-Se group compared to Abx group (Figure S2). When groups were compared in pairs, the antibiotic treatment induced the reduction of the relative abundance of *Lactobacillus* ($p<0.001$) and several *Ruminococcaceae* groups, including *Ruminococcaceae_UCG014* ($p<0.001$) and *Ruminococaceae_UCG010* ($p<0.001$) or *Ruminococaceae_UCG005* ($p=0.002$) and an enrichment in *Parabacteroides* genus ($p<0.001$). However, the supplementation of Se after the antibiotic treatment (Abx vs Abx-Se) induced the increase of *Lactobacillus* ($p<0.001$) and the reduction of *Paracteroides* ($p<0.001$) genus to control levels (no differences in these genera between C and Abx-Se groups).

The genus *Lactobacillus* has been associated with potential beneficial impact on the host, and most of the *Lactobacillus* species and strains have been considered as probiotic.[47] *Lactobacillus* group has been observed in higher abundance in mice groups supplemented with Se, even in the

antibiotic microbiota-depleted group. In this regard, it has been shown that *Lactobacillus* group was increased in diets with median and high Se doses.[43] In addition, the increase of *Lactobacillus* genus has also been reported in mice fed high fat diet supplemented with Se compared with un-supplemented group.[41] Thus, while *Lactobacillus* is significantly reduced in antibiotic treated mice, the Se-supplementation modulated the impact on the *Lactobacillus* levels in similar levels than control groups (groups Abx-Se and C). In agreement with our data, it has been reported that Se-enriched probiotics (0.3 mg kg^{-1} added to a fermentation medium containing the two probiotic strains of microorganisms, *Lactobacillus acidophilus* and *Saccharomyces cerevisiae*) affects pig microbiota composition towards an increase abundance on *Lactobacillus* groups and a decrease on *Escherichia coli* abundance.[48] Other *in vivo* study also reported the effect of Se-containing green tea in the viability and growth of lactic acid bacteria and bifidobacteria.[49] In the same line, other study reported the positive impact of Se nanoparticles in poultry feed on the levels of potential beneficial bacteria as *Faecalibacterium prausnitzii*, *Lactobacillus* spp. and *Ruminococcus* spp. as well as the total short-chain fatty acids (SCFAs), in particular the increase of butyric acid.[50] *Ruminococcaceae_UCG014* has been linked with Se-yeast supplemented laying hens and it is a common family related with the maintenance of gut health and had the enzymatic ability to degrade cellulose and hemicellulose.[51] Other study also reported the impact of supplementation of inorganic Se in dogs on the enrichment of family *Ruminococcaceae*, including the genera *Catenibacterium, Holdemanella* and *Ruminococcaceae UCG-014*, and also, organic Se increased the presence of *Lactobacillus* genus and decreased the presence of *Escherichia coli* (Proteobacteria phylum).[52] Our results showed an increase on *Christensenellaceae* members on the Se group of conventional mice. This microbial group has been described as a highly heritable microbe in humans and it has been also associated with

357 health[53] and inversely related to host body mass index (BMI) in different populations and
358 multiple studies. Although we observed that Se-supplementation increased the relative
359 abundance of *Christensellaceae* group, antibiotics caused a dramatically reduction of these
360 bacteria, which cannot be modulated by Se. Studies using GF mice fed Se-supplementation (0.4
361 mg Se kg^{-1}) showed a potential beneficial impact on microbial diversity[14] in a similar manner
362 than CV. Thus, it has been suggested the potential effect of Se-supplementation on the gut
363 microbiota modulation. Although the mechanisms by which Se shape gut microbiota bacteria are
364 complex, we have reported the potential benefit in the gut microbiota even when microbiota was
365 depleted with antibiotics groups. Our observations highlight three important results: (i)
366 significant stimulation of potential beneficial bacteria as *Lactobacillus, Ruminoccocaceae* and
367 *Christensellaceae* members, (ii) significant increase on microbial diversity and (iii) richness.
368 Further studies would be necessary to understand the exact mechanisms of microbiota-Se
369 interactions and the potential benefits for health.
370 Furthermore, despite the evidence on the impact of Se or specific enriched Se-foods on specific
371 microbial groups[9,14,54], little is known about the impact on selenoproteome profile.
372 **Associations between Gut Microbiota and Selenoproteome in Plasma**
373 As potential links between gut microbiota metabolism and plasma selenoproteome, we
374 investigated the potential associations between gut microbial taxa and the plasma
375 selenoproteome profile in the studied groups C, C-Se, Abx and Abx-Se (Table S6). A significant
376 reduced number of associations were observed in the microbiota depleted mice (Abx) explained
377 by the reduction in microbial diversity and richness. In this sense, only higher *Lactobacillus*
378 (rho=0.71, p=0.03) and *Lachnospiraceae_UCG-01* (rho=0.79, p=0.03) were associated with
379 higher SEPP1 in Abx (Figure 5a). On the contrary, the number of correlations between bacteria

and selenoproteins increased significantly after Se supplementation in Abx-Se (Figure 5b) suggesting again the intertwined mechanism between Se and microbiota. Interestingly, higher SEPP1 were associated with lower abundance of *Alistipes* (rho=-0.7, p=0.03) and *Ruminoclostridium_6* (rho=-0.71, p=0.02), and higher abundance of *Anaerotruncus* (rho=0.77, p=0.01), *Angekisella* (rho=-0.68, p=0.03), *Family_XII_UCG-001* (rho=0.85, p=0.002), *Prevotellaceae_UCG-001* (rho=0.77, p=0.01), and *Ruminococcus_1* (rho=0.85, p=0.002). On the other hand, the concentration of GPx was positively correlated with *Parvibacter* (rho=0.67, p=0.05) and *Ruminococcaceae_UCG-009* (rho=0.74, p=0.02) and negatively with *Lachnospiraceae_UCG-004* (rho=-0.68, p=0.04) in C group (Figure 5c). No significant correlations of these bacteria with GPx were found in mice with depletion of microbiota (Abx). However, *Parvibacter* (rho=-0.72, p=0.02) were inversely associated with this selenoprotein in mice fed Se-supplemented diet (C-Se) and microbiota depleted mice fed Se-supplemented diet (Abx-Se) respectively. In the same way, positive correlations between SeAlb and *Lachnospiraceae_UCG-001* were observed in C (rho=0.82, p=0.02) and Abx-Se (rho=0.73, p=0.02), but no associations in Abx were found. Finally, in terms of diversity, only the Abx-Se group showed significant associations. In this group, GPx was positively correlated with Shannon index (rho=0.69, p=0.029) and SeAlb with Chao1 index (R=0.66, p=0.038).

Associations between Trace Elements Homeostasis in Plasma and Gut Microbiota according to Se-supplementation and Antibiotic-Microbiota Disruption

Correlation analysis between total elements in plasma and genus were reported for the first time. Our results showed that Al, Co, Cu, Mn, V and Zn correlated with different genera in C, C-Se, Abx and Abx-Se (Table S7). Per groups, Abx-Se showed the highest number of associations with genus (11 significant correlations) especially with Al, followed by C and C-Se, which presented

a total of 7 significant correlations per group. However, no correlations between elements and genera were found in Abx group. This fact may indicate the intertwined role of Se and gut microbiota in metal homeostasis, which is in good agreement with the previously discussed results. In this sense, *Enterorhabdus* (rho=-0.88, p=0.01), *Erysipelatoclostridium* (rho=-0.63, p=0.04) and *Ruminococcaceae_UCG-010* (rho=-0.82, p=0.02) were negatively associated with Al in Abx-Se group. Moreover, higher *Flavonifractor* (rho=0.78, p=0.01) and *Ruminiclostridium_9* (rho=0.75, p=0.02) were associated with higher Al. In addition, we found that higher *Subdoligranulum* (rho=0.71, p=0.02) correlated with higher V in the same group. In C-Se group, *Prevotellaceae_UCG-001* (rho=0.85, p=0.03) and *Ruminiclostridium* (rho=0.87, p=0.01) were positively correlated with Mn. Finally, we observed that Co was positively associated with *Acetifactor* in C-Se but negatively in Abx-Se.

In summary, we can conclude that plasma selenoproteome and metal homeostasis were considerably affected by Se-supplementation, possibly by the interplay between Se and gut microbiota. Our study demonstrated the potential beneficial effects of Se on the gut microbiota, especially after microbiota depletion by antibiotics, as well as the associations of specific bacteria with plasma selenoproteins: GPx, SEPP1 and SeAlb and the concentrations of some elements. However, further studies are needed to identify the specific Se-microbiota interactions and the potential implication in health outcomes.

425

426 **Supporting Information Description**

427 Table S1. Reproducibility of the analysis using Human Serum BCR-637 certified reference
428 material

429 Table S2. Reproducibility of the analysis ICP-QQQ-MS using Clinchek, Serum Level II as
430 control for trace elements.

431 Table S3. Relative abundances at phylum level for each group. P-value from Wilcoxon test with
432 False Discovery test Rate (FDR).

433 Table S4. Relative abundances at family level for each group. P-value from Wilcoxon test with
434 False Discovery test Rate (FDR).

435 Table S5. Relative abundances at genus level for each group. P-value from Wilcoxon test with
436 False Discovery test Rate (FDR).

437 Table S6. Spearman correlation coefficients between metals and genus. Only significant
438 correlation coefficients ($p<0.05$) are shown in the table. **Genus correlated with the same
439 element in two groups at least. N.S.: Non-significant.

440 Table S7. Spearman correlation coefficients between selenoproteins and genus. Only significant
441 correlation coefficients ($p<0.05$) are shown in the table. **Genus correlated with selenoproteins
442 in two groups at least. N.S.: Non-significant.

443 Figure S1. Number of sequences at a) group level and b) individual level. No differences in the
444 sequencing coverage were observed between groups.

Figure S2. Boxplot of abundance corresponding to genera with significant differences in Wilcoxon test with False Discovery test Rate (FDR).

Figure S3. Linear Discriminant Analysis (LDA) Effect Size (LEfSe) plot of taxonomic biomarkers identified in the gut microbiota of different groups at genus levels and compared between groups. The LEfSe algorithm, emphasizing both statistical and biological relevance, was used for biomarker discovery. The threshold for the logarithmic discriminant analysis (LDA) score was 3.0

REFERENCES

(1) Lü, J.; Zhang, J.; Jiang, C.; Deng, Y.; Özten, N.; Bosland, M. C. Cancer Chemoprevention Research with Selenium in the Post-SELECT Era: Promises and Challenges. *Nutr. Cancer* **2016**, *68* (1), 1–17. https://doi.org/10.1080/01635581.2016.1105267.

(2) Benstoem, C.; Goetzenich, A.; Kraemer, S.; Borosch, S.; Manzanares, W.; Hardy, G.; Stoppe, C. Selenium and Its Supplementation in Cardiovascular Disease--What Do We Know? *Nutrients* **2015**, *7* (5), 3094–3118. https://doi.org/10.3390/nu7053094.

(3) Pedrero, Z.; Madrid, Y. Novel Approaches for Selenium Speciation in Foodstuffs and Biological Specimens: A Review. *Anal. Chim. Acta* **2009**, *634* (2), 135–152. https://doi.org/10.1016/j.aca.2008.12.026.

(4) Rayman, M. P. Selenium and Human Health. *The Lancet*. March 2012, pp 1256–1268. https://doi.org/10.1016/S0140-6736(11)61452-9.

(5) Gómez-Jacinto, V.; Navarro-Roldán, F.; Garbayo-Nores, I.; Vílchez-Lobato, C.; Borrego, A. A.; García-Barrera, T. In Vitro Selenium Bioaccessibility Combined with in Vivo Bioavailability and Bioactivity in Se-Enriched Microalga (Chlorella Sorokiniana) to Be Used as Functional Food. *J. Funct. Foods* **2020**, *66*, 103817.

https://doi.org/10.1016/j.jff.2020.103817.

(6) Gómez-Jacinto, V.; Navarro-Roldán, F.; Garbayo-Nores, I.; Vílchez-Lobato, C.; Borrego, A. A.; García-Barrera, T. In Vitro Selenium Bioaccessibility Combined with in Vivo Bioavailability and Bioactivity in Se-Enriched Microalga (Chlorella Sorokiniana) to Be Used as Functional Food. *J. Funct. Foods* **2020**, *66*, 103817. https://doi.org/https://doi.org/10.1016/j.jff.2020.103817.

(7) Yang, Q.; Liang, Q.; Balakrishnan, B.; Belobrajdic, D. P.; Feng, Q.-J.; Zhang, W. Role of Dietary Nutrients in the Modulation of Gut Microbiota: A Narrative Review. *Nutrients* . 2020. https://doi.org/10.3390/nu12020381.

(8) Sircana, A.; Framarin, L.; Leone, N.; Berrutti, M.; Castellino, F.; Parente, R.; De Michieli, F.; Paschetta, E.; Musso, G. Altered Gut Microbiota in Type 2 Diabetes: Just a Coincidence? *Curr. Diab. Rep.* **2018**, *18* (10), 98. https://doi.org/10.1007/s11892-018-1057-6.

(9) Zhai, Q.; Cen, S.; Li, P.; Tian, F.; Zhao, J.; Zhang, H.; Chen, W. Effects of Dietary Selenium Supplementation on Intestinal Barrier and Immune Responses Associated with Its Modulation of Gut Microbiota. *Environ. Sci. Technol. Lett.* **2018**, *5* (12), 724–730. https://doi.org/10.1021/acs.estlett.8b00563.

(10) De Filippis, F.; Vitaglione, P.; Cuomo, R.; Berni Canani, R.; Ercolini, D. Dietary Interventions to Modulate the Gut Microbiome-How Far Away Are We From Precision Medicine. *Inflamm. Bowel Dis.* **2018**, *24* (10), 2142–2154. https://doi.org/10.1093/ibd/izy080.

(11) Hrdina, J.; Banning, A.; Kipp, A.; Loh, G.; Blaut, M.; Brigelius-Flohé, R. The Gastrointestinal Microbiota Affects the Selenium Status and Selenoprotein Expression in

Mice. *J. Nutr. Biochem.* **2009**, *20* (8), 638–648. https://doi.org/10.1016/j.jnutbio.2008.06.009.

(12) Takahashi, K.; Suzuki, N.; Ogra, Y. Effect of Gut Microflora on Nutritional Availability of Selenium. *Food Chem.* **2020**, *319* (December 2018), 1–8. https://doi.org/10.1016/j.foodchem.2020.126537.

(13) Liu, Y.; Ji, J.; Zhang, W.; Suo, Y.; Zhao, J.; Lin, X.; Cui, L.; Li, B.; Hu, H.; Chen, C.; Li, Y.-F. Selenium Modulated Gut Flora and Promoted Decomposition of Methylmercury in Methylmercury-Poisoned Rats. *Ecotoxicol. Environ. Saf.* **2019**, *185*, 109720. https://doi.org/https://doi.org/10.1016/j.ecoenv.2019.109720.

(14) Kasaikina, M. V.; Kravtsova, M. A.; Lee, B. C.; Seravalli, J.; Peterson, D. A.; Walter, J.; Legge, R.; Benson, A. K.; Hatfield, D. L.; Gladyshev, V. N. Dietary Selenium Affects Host Selenoproteome Expression by Influencing the Gut Microbiota. *FASEB J.* **2011**, *25* (7), 2492–2499. https://doi.org/10.1096/fj.11-181990.

(15) Plummer, J. D.; Postnikoff, S. D.; Tyler, J. K.; Johnson, J. E. Selenium Supplementation Inhibits IGF-1 Signaling and Confers Methionine Restriction-like Healthspan Benefits to Mice. *Elife* **2021**, *10*, e62483. https://doi.org/10.7554/eLife.62483.

(16) Zhai, Q.; Xiao, Y.; Li, P.; Tian, F.; Zhao, J.; Zhang, H.; Chen, W. Varied Doses and Chemical Forms of Selenium Supplementation Differentially Affect Mouse Intestinal Physiology. *Food Funct.* **2019**, *10* (9), 5398–5412. https://doi.org/10.1039/c9fo00278b.

(17) Morales-Prieto, N.; Ruiz-Laguna, J.; Abril, N. Dietary Se Supplementation Partially Restores the REDOX Proteomic Map of M. Spretus Liver Exposed to P,p′-DDE. *Food Chem. Toxicol.* **2018**, *114*, 292–301. https://doi.org/10.1016/j.fct.2018.02.047.

(18) García-Sevillano, M. A.; Rodríguez-Moro, G.; García-Barrera, T.; Navarro, F.; Gómez-

Ariza, J. L. Biological Interactions between Mercury and Selenium in Distribution and Detoxification Processes in Mice under Controlled Exposure. Effects on Selenoprotein. *Chem. Biol. Interact.* **2015**, *229*, 82–90. https://doi.org/10.1016/j.cbi.2015.02.001.

(19) Zarrinpar, A.; Chaix, A.; Xu, Z. Z.; Chang, M. W.; Marotz, C. A.; Saghatelian, A.; Knight, R.; Panda, S. Antibiotic-Induced Microbiome Depletion Alters Metabolic Homeostasis by Affecting Gut Signaling and Colonic Metabolism. *Nat. Commun.* **2018**, *9* (1), 2872. https://doi.org/10.1038/s41467-018-05336-9.

(20) Reikvam, D. H.; Erofeev, A.; Sandvik, A.; Grcic, V.; Jahnsen, F. L.; Gaustad, P.; McCoy, K. D.; Macpherson, A. J.; Meza-Zepeda, L. A.; Johansen, F.-E. Depletion of Murine Intestinal Microbiota: Effects on Gut Mucosa and Epithelial Gene Expression. *PLoS One* **2011**, *6* (3), e17996. https://doi.org/10.1371/journal.pone.0017996.

(21) D'Amato, A.; Di Cesare Mannelli, L.; Lucarini, E.; Man, A. L.; Le Gall, G.; Branca, J. J. V; Ghelardini, C.; Amedei, A.; Bertelli, E.; Regoli, M.; Pacini, A.; Luciani, G.; Gallina, P.; Altera, A.; Narbad, A.; Gulisano, M.; Hoyles, L.; Vauzour, D.; Nicoletti, C. Faecal Microbiota Transplant from Aged Donor Mice Affects Spatial Learning and Memory via Modulating Hippocampal Synaptic Plasticity- and Neurotransmission-Related Proteins in Young Recipients. *Microbiome* **2020**, *8* (1), 140. https://doi.org/10.1186/s40168-020-00914-w.

(22) Callejón-Leblic, B.; Rodríguez-Moro, G.; Arias-Borrego, A.; Pereira -Vega A;Gómez-Ariza J.L; García-Barrera, T. Absolute Quantification of Selenoproteins and Selenometabolites in Lung Cancer Human Serum by Column Switching Coupled to Triple Quadrupole Inductively Coupled Plasma Mass Spectrometry. *J. Chromatogr. A* **2020**, *1619*, 460919.

(23) Sanguinetti, E.; Guzzardi, M. A.; Tripodi, M.; Panetta, D.; Selma-Royo, M.; Zega, A.; Telleschi, M.; Collado, M. C.; Iozzo, P. Microbiota Signatures Relating to Reduced Memory and Exploratory Behaviour in the Offspring of Overweight Mothers in a Murine Model. *Sci. Rep.* **2019**, *9* (1), 12609. https://doi.org/10.1038/s41598-019-48090-8.

(24) Bolger, A. M.; Lohse, M.; Usadel, B. Trimmomatic: A Flexible Trimmer for Illumina Sequence Data. *Bioinformatics* **2014**, *30* (15), 2114–2120. https://doi.org/10.1093/bioinformatics/btu170.

(25) Callahan, B. J.; McMurdie, P. J.; Rosen, M. J.; Han, A. W.; Johnson, A. J. A.; Holmes, S. P. DADA2: High-Resolution Sample Inference from Illumina Amplicon Data. *Nat. Methods* **2016**, *13* (7), 581–583. https://doi.org/10.1038/nmeth.3869.

(26) Quast, C.; Pruesse, E.; Yilmaz, P.; Gerken, J.; Schweer, T.; Yarza, P.; Peplies, J.; Glöckner, F. O. The SILVA Ribosomal RNA Gene Database Project: Improved Data Processing and Web-Based Tools. *Nucleic Acids Res.* **2013**, *41* (Database issue), D590-6. https://doi.org/10.1093/nar/gks1219.

(27) Yilmaz, P.; Parfrey, L. W.; Yarza, P.; Gerken, J.; Pruesse, E.; Quast, C.; Schweer, T.; Peplies, J.; Ludwig, W.; Glöckner, F. O. The SILVA and "All-Species Living Tree Project (LTP)" taxonomic Frameworks. *Nucleic Acids Res.* **2014**, *42* (Database issue), D643-8. https://doi.org/10.1093/nar/gkt1209.

(28) R Core Team (2020). R: A language and environment for statistical computing. R Foundation for Statistical Computing, Vienna, A. R Core Team (2020).

(29) Zakrzewski, M.; Proietti, C.; Ellis, J. J.; Hasan, S.; Brion, M.-J.; Berger, B.; Krause, L. Calypso: A User-Friendly Web-Server for Mining and Visualizing Microbiome-Environment Interactions. *Bioinformatics* **2017**, *33* (5), 782–783.

https://doi.org/10.1093/bioinformatics/btw725.

(30) Morris, J. S.; Crane, S. B. Selenium Toxicity from a Misformulated Dietary Supplement, Adverse Health Effects, and the Temporal Response in the Nail Biologic Monitor. *Nutrients* **2013**, *5* (4), 1024–1057. https://doi.org/10.3390/nu5041024.

(31) Zhang, L.; Zeng, H.; Cheng, W.-H. Beneficial and Paradoxical Roles of Selenium at Nutritional Levels of Intake in Healthspan and Longevity. *Free Radic. Biol. Med.* **2018**, *127*, 3–13. https://doi.org/https://doi.org/10.1016/j.freeradbiomed.2018.05.067.

(32) Rodríguez-González, P.; Rodríguez-Cea, A.; Alonso, J. I. G.; Sanz-Medel, A. Species-Specific Isotope Dilution Analysis and Isotope Pattern Deconvolution for Butyltin Compounds Metabolism Investigations. *Anal. Chem.* **2005**, *77* (23), 7724–7734. https://doi.org/10.1021/ac051091r.

(33) Mostert, V. Selenoprotein P: Properties, Functions, and Regulation. *Arch. Biochem. Biophys.* **2000**, *376* (2), 433–438. https://doi.org/10.1006/abbi.2000.1735.

(34) Combs Jr, G. F. Biomarkers of Selenium Status. *Nutrients* **2015**, *7* (4), 2209–2236. https://doi.org/10.3390/nu7042209.

(35) Burk, R. F.; Hill, K. E.; Motley, A. K. Selenoprotein Metabolism and Function: Evidence for More than One Function for Selenoprotein P. *J. Nutr.* **2003**, *133* (5 SUPPL. 2).

(36) Burk, R. F.; Hill, K. E. Selenoprotein P-Expression, Functions, and Roles in Mammals. *Biochim. Biophys. Acta* **2009**, *1790* (11), 1441–1447.

(37) Björnstedt M, Xue J, Huang W, Akesson B, H. A. The Thioredoxin and Glutaredoxin Systems Are Efficient Electron Donors to Human Plasma Glutathione Peroxidase. **1994**, *269*, 29382–29382.

(38) García-Barrera, T.; Gómez-Ariza, J. L.; González-Fernández, M.; Moreno, F.; García-

583 Sevillano, M. A.; Gómez-Jacinto, V. Biological Responses Related to Agonistic,
584 Antagonistic and Synergistic Interactions of Chemical Species. *Anal. Bioanal. Chem.*
585 **2012**, *403* (8), 2237–2253. https://doi.org/10.1007/s00216-012-5776-2.
586 (39) Garcia Sevillano, M.; Rodríguez-Moro, G.; García-Barrera, T.; Navarro, F.; Gomez-Ariza,
587 J. L. Biological Interactions between Mercury and Selenium in Distribution and
588 Detoxification Processes in Mice under Controlled Exposure. Effects on Selenoprotein.
589 *Chem. Biol. Interact.* **2015**, *229*. https://doi.org/10.1016/j.cbi.2015.02.001.
590 (40) Rodríguez-Moro, G.; Roldán, F. N.; Baya-Arenas, R.; Arias-Borrego, A.; Callejón-Leblic,
591 B.; Gómez-Ariza, J. L.; García-Barrera, T. Metabolic Impairments, Metal Traffic, and
592 Dyshomeostasis Caused by the Antagonistic Interaction of Cadmium and Selenium Using
593 Organic and Inorganic Mass Spectrometry. *Environ. Sci. Pollut. Res. Int.* **2020**, *27* (2),
594 1762–1775. https://doi.org/10.1007/s11356-019-06573-1.
595 (41) Yu, T.; Guo, J.; Zhu, S.; Li, M.; Zhu, Z.; Cheng, S.; Wang, S.; Sun, Y.; Cong, X.
596 Protective Effects of Selenium-Enriched Peptides from Cardamine Violifolia against
597 High-Fat Diet Induced Obesity and Its Associated Metabolic Disorders in Mice. *RSC Adv.*
598 **2020**, *10* (52), 31411–31424. https://doi.org/10.1039/D0RA04209A.
599 (42) Rizzatti, G.; Lopetuso, L. R.; Gibiino, G.; Binda, C.; Gasbarrini, A. Proteobacteria: A
600 Common Factor in Human Diseases. *Biomed Res. Int.* **2017**, *2017*, 9351507.
601 https://doi.org/10.1155/2017/9351507.
602 (43) Xie, D.; Jiang, L.; Lin, Y.; Liu, Z. Antioxidant Activity of Selenium-Enriched Chrysomyia
603 Megacephala (Fabricius) Larvae Powder and Its Impact on Intestinal Microflora in D-
604 Galactose Induced Aging Mice. *BMC Complement. Med. Ther.* **2020**, *20* (1), 264.
605 https://doi.org/10.1186/s12906-020-03058-4.

(44) Hall, J. A.; Isaiah, A.; Estill, C. T.; Pirelli, G. J.; Suchodolski, J. S. Weaned Beef Calves Fed Selenium-Biofortified Alfalfa Hay Have an Enriched Nasal Microbiota Compared with Healthy Controls. *PLoS One* **2017**, *12* (6). https://doi.org/10.1371/journal.pone.0179215.

(45) Denton, K.; Atkinson, M. M.; Borenstein, S. P.; Carlson, A.; Carroll, T.; Cullity, K.; Demarsico, C.; Ellowitz, D.; Gialtouridis, A.; Gore, R.; Herleikson, A.; Ling, A. Y.; Martin, R.; McMahan, K.; Naksukpaiboon, P.; Seiz, A.; Yearwood, K.; O'Neill, J.; Wiatrowski, H. Identification of a Possible Respiratory Arsenate Reductase in Denitrovibrio Acetiphilus, a Member of the Phylum Deferribacteres. *Arch. Microbiol.* **2013**, *195* (9), 661–670. https://doi.org/10.1007/s00203-013-0915-5.

(46) Takai, K.; Kobayashi, H.; Nealson, K. H.; Horikoshi, K. Deferribacter Desulfuricans Sp. Nov., a Novel Sulfur-, Nitrate- and Arsenate-Reducing Thermophile Isolated from a Deep-Sea Hydrothermal Vent. *Int. J. Syst. Evol. Microbiol.* **2003**, *53* (Pt 3), 839–846. https://doi.org/10.1099/ijs.0.02479-0.

(47) Reid, G. The Scientific Basis for Probiotic Strains of Lactobacillus. *Appl. Environ. Microbiol.* **1999**, *65* (9), 3763–3766.

(48) Lv, C. H.; Wang, T.; Regmi, N.; Chen, X.; Huang, K.; Liao, S. F. Effects of Dietary Supplementation of Selenium-Enriched Probiotics on Production Performance and Intestinal Microbiota of Weanling Piglets Raised under High Ambient Temperature. *J. Anim. Physiol. Anim. Nutr. (Berl).* **2015**, *99* (6), 1161–1171. https://doi.org/10.1111/jpn.12326.

(49) Molan, A. L.; Flanagan, J.; Wei, W.; Moughan, P. J. Selenium-Containing Green Tea Has Higher Antioxidant and Prebiotic Activities than Regular Green Tea. *Food Chem.* **2009**,

114 (3), 829–835. https://doi.org/10.1016/j.foodchem.2008.10.028.

(50) Gangadoo, S.; Dinev, I.; Chapman, J.; Hughes, R. J.; Van, T. T. H.; Moore, R. J.; Stanley, D. Selenium Nanoparticles in Poultry Feed Modify Gut Microbiota and Increase Abundance of Faecalibacterium Prausnitzii. *Appl. Microbiol. Biotechnol.* **2018**, *102* (3), 1455–1466. https://doi.org/10.1007/s00253-017-8688-4.

(51) zhexi liu, yutao cao, yue ai, linli wang, mengyao wang, bingkun zhang, yuming guo, zhengxing lian, keliang wu, hongbing han. Selenium Yeast Modulated Ileal Transcriptome and Microbiota to Ameliorate Egg Production in Aged Laying Hens. *Res. Sq.* **2020**, *Pre-print*, 1–31.

(52) Pereira, A. M.; Pinna, C.; Biagi, G.; Stefanelli, C.; Maia, M. R. G.; Matos, E.; Segundo, M. A.; Fonseca, A. J. M.; Cabrita, A. R. J. Supplemental Selenium Source on Gut Health: Insights on Fecal Microbiome and Fermentation Products of Growing Puppies. *FEMS Microbiol. Ecol.* **2020**, *96* (11). https://doi.org/10.1093/femsec/fiaa212.

(53) Waters, J. L.; Ley, R. E. The Human Gut Bacteria Christensenellaceae Are Widespread, Heritable, and Associated with Health. *BMC Biol.* **2019**, *17* (1), 83. https://doi.org/10.1186/s12915-019-0699-4.

(54) Gao, Y.; Xu, Y.; Ruan, J.; Yin, J. Selenium Affects the Activity of Black Tea in Preventing Metabolic Syndrome in High-Fat Diet-Fed Sprague-Dawley Rats. *J. Sci. Food Agric.* **2020**, *100* (1), 225–234. https://doi.org/10.1002/jsfa.10027.

Funding Sources

This work was supported by the projects PG2018-096608-B-C21 from the Spanish Ministry of Science and innovation (MINECO) and UHU-1256905 from the FEDER Andalusian Operative Program 2014-2020 (Ministry of Economy, Knowledge, Business and Universities, Regional Government of Andalusia, Spain). Authors would like to acknowledge the support from The Ramón Areces Foundation (ref. CIVP19A5918). Authors are grateful to FEDER (European Community) for financial support, Grant UNHU13-1E-1611.

AUTHOR INFORMATION

Corresponding Author

*T. García Barrera. Research Center of Natural Resources, Health and the Environment (RENSMA). Department of Chemistry, Faculty of Experimental Sciences, University of Huelva, Fuerzas Armadas Ave., 21007, Huelva, Spain; Tel.: +34 959219962; E-mail: tamara@dqcm.uhu.es. Σ Senior authors.

Author Contributions

The manuscript was written through contributions of all authors. All authors have given approval to the final version of the manuscript.

ABBREVIATIONS: Abx, antibiotic treated mice fed rodent diet; Abx-Se, antibiotic treated mice fed Se-supplementation diet; AF, affinity chromatography; C, control mice fed rodent diet; C-Se, mice fed Se-Supplementation diet; CV, conventional mice; GF, Germ Free mice; GPx, plasma glutathione peroxidase; ICP-QQQ-MS, inductively coupled plasma mass spectrometry with triple quadrupole; LDA, Linear Discriminant Analysis, LEfSe, Effect Size (LEfSe) plot,

PCoA, Principal Coordinate Analyses; RDA, Multivariate redundant discriminant analysis; SeAlb, selenoalbumine; SEC, size exclusion chromatography; SEPP1, selenoprotein P.

673 **Figure Captions**

674 **Figure 1.** Experimental design showing the studied groups.

675 **Figure 2.** Mass flow chromatograms corresponding to (a) BCR-637 fortified with 50 ng g^{-1} of
676 selenite and (b) plasma mice after speciation of selenoproteins.

677 **Figure 3.** Model map showing the mechanism underlying the potential beneficial effects of Se in
678 the conditions with and without antibiotics.

679 **Figure 4.** Impact of Se-supplementation on the microbiota of control mice and microbiota
680 depleted mice. a) PCoA of bacterial beta-diversity based on the Bray Curtis distance (p-
681 value=0.0003). b) Multivariate RDA showed significant microbiota among groups (p-
682 value=0,001). Box plots showing alpha diversity c) Chao1 richness estimator and d) Shannon
683 Index. e) LDA LEfSe plot of taxonomic biomarkers identified in the gut microbiota of different
684 groups at family levels. The LDA score threshold was 3. f) Boxplots of relative abundance of
685 phylum.

686 **Figure 5**. Spearman correlation matrix heatmaps for mice plasma selenoproteins and gut
687 microbiota genus in a) Abx group, b) Abx-Se group, c) C group and d) C-Se group.

688

689

Tables

Table 1. Average concentration of selenium in selenoproteins, total selenium and fold changes.

Selenoproteins					
Groups	GPx	Selenometabolites	SEPP1	SeAlb	Total Se
Concentration (ng of selenium per g of plasma) ± S.E.M (n=10 mice per group)					
C	15.4±1.8	<LOD	381.1±11.7	27.8±2.4	434.5±14.3
C-Se	28.3±2.3	<LOD	414.0±22.0	49.3±5.7	509.0±28.6
Abx	22.3±1.1	<LOD	401.2±17.7	50.7±3.0	483.2±17.7
Abx-Se	28.0±1.5	<LOD	398.6±18.3	46.8±4.1	489.3±18.8
Fold change					
C-Se/C	1.84 (p<0.001)	-	1.09	1.77 (p<0.003)	1.16
Abx/C	1.44 (p<0.04)	-	1.05	1.82 (p<0.002)	1.12
Abx-Se/C	1.82 (p<0.001)	-	1.05	1.68 (p<0.01)	1.12
Abx-Se/Abx	1.26	-	0.99	0.92	1.00

LD: Detection Limit of selenometabolites 0.5 ng Se g^{-1}; p: p-value from ANOVA followed by Tukey Test (only significant p-values are shown in the table). p<0.05 was considered statistically significant

Table 2. Metal profile in mice plasma

Elements	Average Concentration ± S.E.M				Fold changes			
	C	C-Se	Abx	Abx-Se	C-Se/C	Abx-Se/C	Abx-Se/C-Se	Abx-Se/Abx
Al	25.4 ± 2.9	39.0 ± 4.3	24.2 ± 2.9	23.4 ± 2.7	1.54(p=0.03)	0.92	0.60 (*p*=0.01)	0.97
V	10.4 ± 0.8	13.6 ± 1.4	9.7 ± 0.7	9.1 ± 1.1	1.31	0.87	0.67 (*p*=0.03)	0.94
Cr	7.6 ± 0.7	11.1 ± 1.7	7.7 ± 0.5	7.3 ± 1.1	1.45	0.95	0.66	0.94
Mn	5.6 ± 0.5	8.2 ± 1.8	7.3 ± 1.1	7.4 ± 1.9	1.45	1.32	0.91	1.02
Fe	7448 ±1264	6504 ±1412	6099 ± 946	6108 ± 937	0.87	0.82	0.94	1.00
Co	6.2 ± 0.4	6.2 ± 0.5	5.3 ± 0.4	4.7 ± 0.5	1.01	0.76 (*p*=0.01)	0.75 (*p*=0.04)	0.89
Ni	4.5 ± 0.9	6.8 ± 1.3	3.2 ± 0.4	4.2 ± 0.9	1.51	0.92	0.61	1.28
Cu	649± 24	684 ± 33	602 ± 15	584 ± 29	1.05	0.90	0.85 (*p*=0.05)	0.97
Zn	1031 ± 40	1071 ± 38	1014 ± 46	1213 ± 74	1.04	1.18 (*p*=0.04)	1.13	1.20 (*p*=0.03)
As	23.3 ± 3.6	22.2 ± 4.1	20.3 ± 3.0	19.7 ± 2.5	0.95	0.84	0.89	0.97
Mo	29.6 ± 1.6	45.4 ± 5.4	39.8 ± 7.5	33.4 ± 2.9	1.53(*p*=0.03)	1.13	0.74	0.84
Cd	0.12 ± 0.04	0.03 ± 0.01	0.09 ±0.03	0.02 ± 0.01	0.22	0.16	0.74	0.20
Sb	6.7 ± 0.5	9.2 ± 1.1	6.1 ± 0.5	6.7 ± 0.5	1.36	1.00	0.73	1.09
Tl	0.51 ± 0.08	0.70 ± 0.12	0.49 ± 0.08	0.37 ± 0.10	1.37	0.72	0.52	0.74
Pb	2.2 ± 0.2	2.9 ± 0.6	2.7 ± 0.6	2.3 ± 0.4	1.34	1.03	0.77	0.85

Concentrations, fold changes, *p*-values from ANOVA (only significant *p*-values are shown in the table) and standard error of the mean (S.E.M) of the elements. $p<0.05$ was considered statistically significant

Figure graphics

Figure 1. Experimental design showing the studied groups

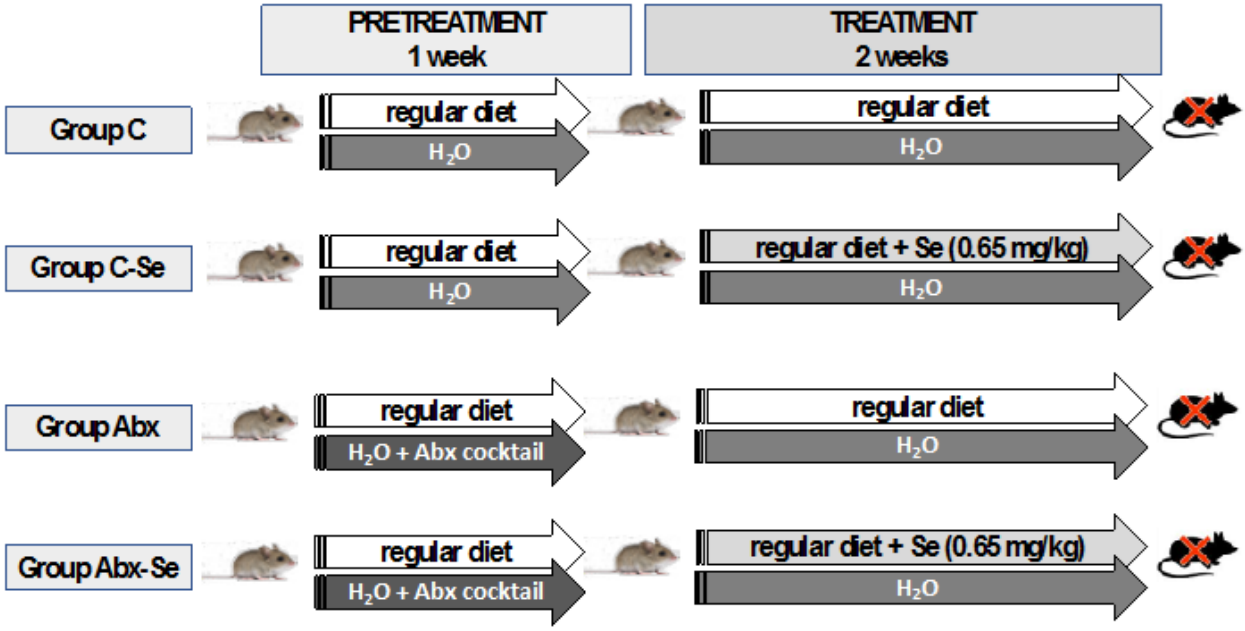

Figure 2. Mass flow chromatograms corresponding to (a) BCR-637 fortified with 50 ng g^{-1} of selenite and (b) plasma mice after speciation of selenoproteins.

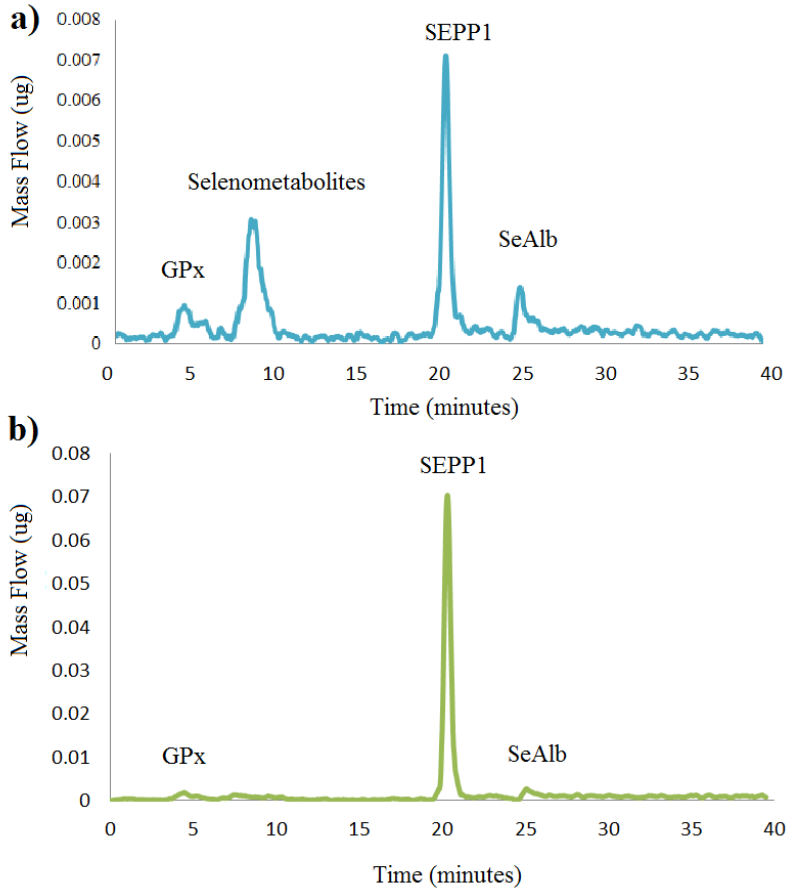

Figure 3. Model map showing the mechanism underlying the potential beneficial effects of Se in the conditions with and without antibiotics.

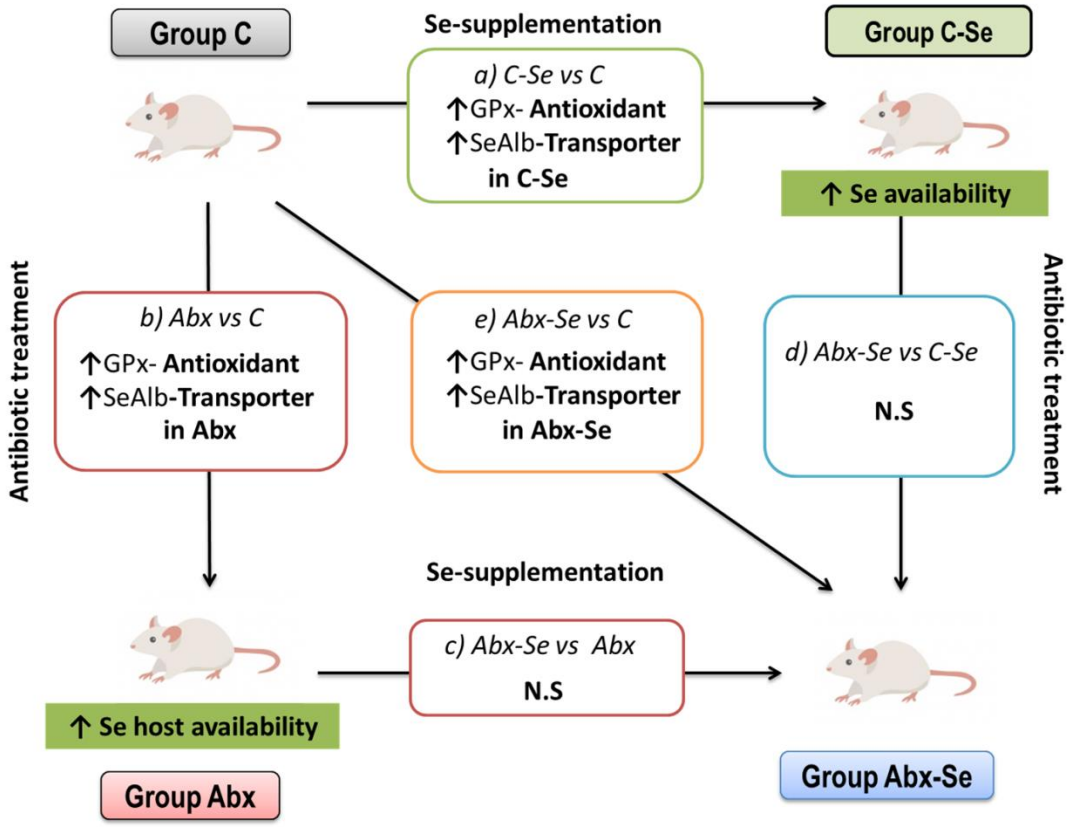

N.S.: Not significant.

Figure 4. Impact of Se-supplementation on the microbiota of control mice and microbiota depleted mice. a) PCoA of bacterial beta-diversity based on the Bray Curtis distance (p-value=0.0003). b) Multivariate RDA showed significant microbiota among groups (p-value=0,001). Box plots showing alpha diversity c) Chao1 richness estimator and d) Shannon Index. e) LDA LEfSe plot of taxonomic biomarkers identified in the gut microbiota of different groups at family levels. The LDA score threshold was 3. f) Boxplots of relative abundance of phylum.

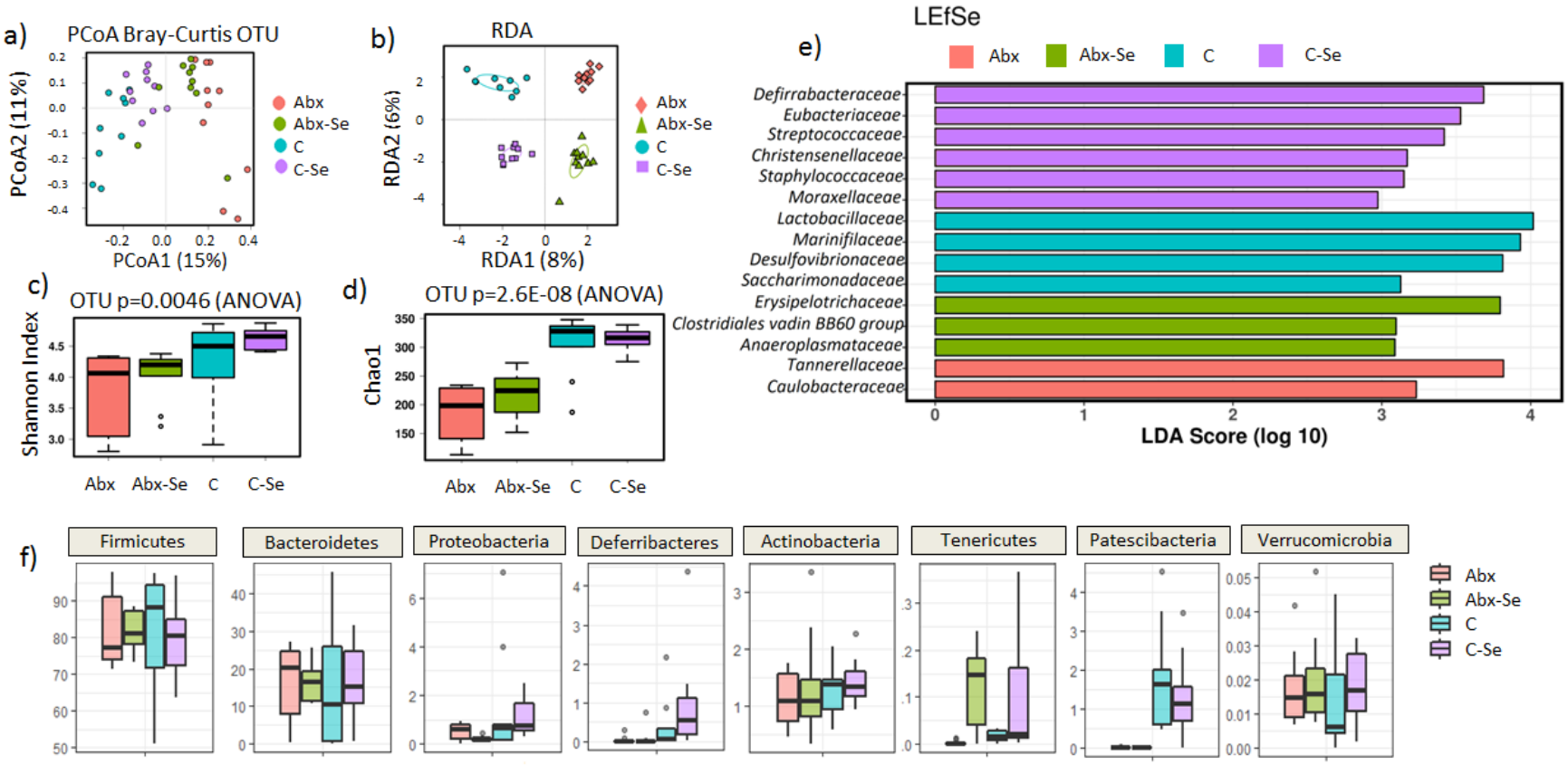
a)
PCoA Bray-Curtis OTU
PCoA2 (11%)
PCoA1 (15%)
Abx
Abx-Se
C
C-Se
b)
RDA
RDA2 (6%)
RDA1 (8%)
c)
OTU p=0.0046 (ANOVA)
Shannon Index
d)
OTU p=2.6E-08 (ANOVA)
Chao1
e)
LEfSe
Defirrabacteraceae
Eubacteriaceae
Streptococcaceae
Christensenellaceae
Staphylococcaceae
Moraxellaceae
Lactobacillaceae
Marinifilaceae
Desulfovibrionaceae
Saccharimonadaceae
Erysipelotrichaceae
Clostridiales vadin BB60 group
Anaeroplasmataceae
Tannerellaceae
Caulobacteraceae
LDA Score (log 10)
f)
Firmicutes
Bacteroidetes
Proteobacteria
Deferribacteres
Actinobacteria
Tenericutes
Patescibacteria
Verrucomicrobia

Figure 5. Spearman correlation matrix heatmaps for mice plasma selenoproteins and gut microbiota genus in a) Abx group, b) Abx-Se group, c) C group and d) C-Se group.

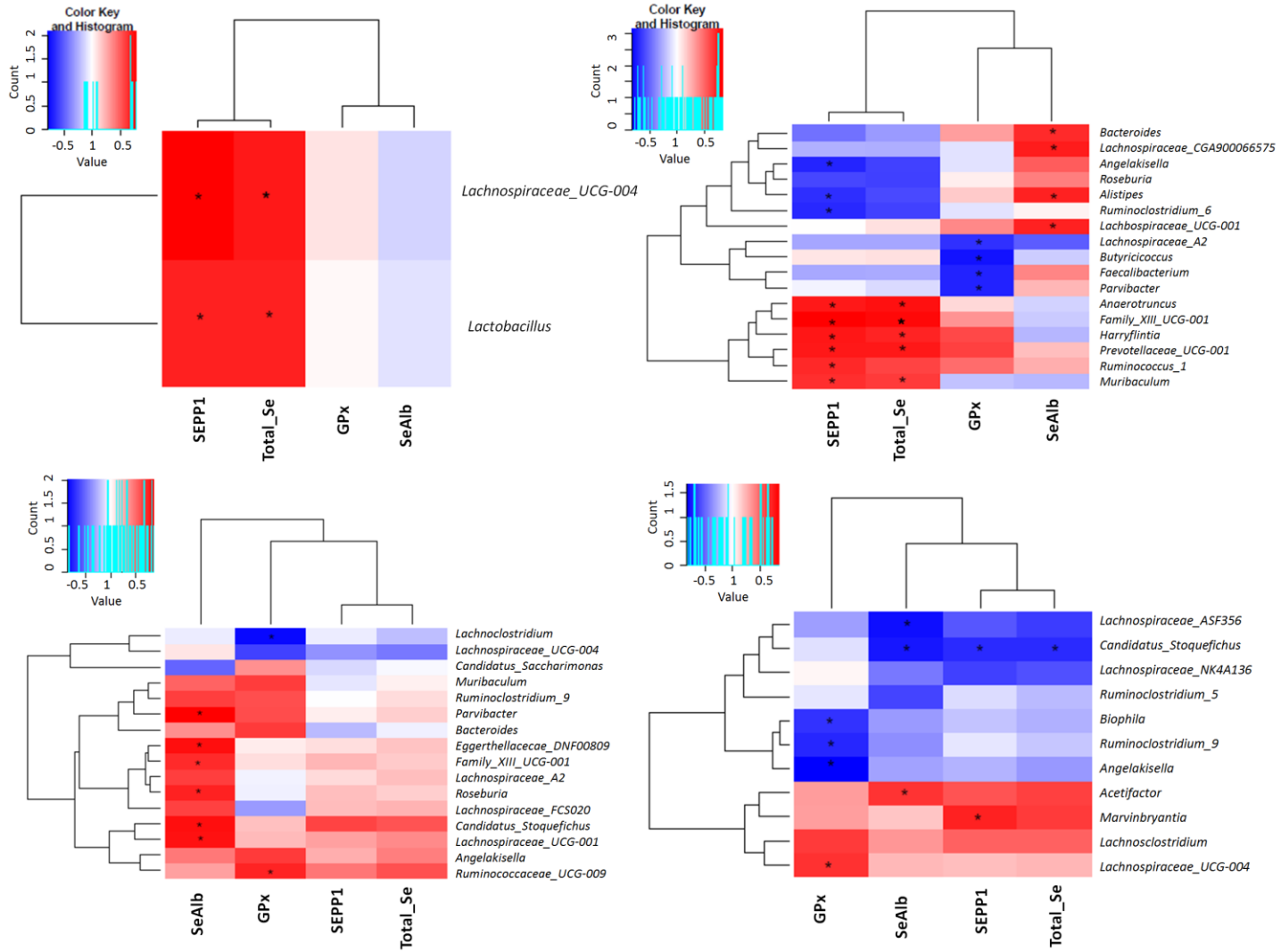

Graphic for table of contents